

A note on the option price and “Mass at zero in the uncorrelated SABR model and implied volatility asymptotics”

Jaehyuk Choi^{a,*}, Lixin Wu^b

^a*Peking University HSBC Business School,
University Town, Nanshan, Shenzhen 518055, China*

^b*Department of Mathematics, The Hong Kong University of Science and Technology,
Clear Water Bay, Kowloon, Hong Kong, China*

Abstract

Gulisashvili et al. [Quant. Finance, 2018, 18(10), 1753–1765] provide a small-time asymptotics for the mass at zero under the uncorrelated SABR model by approximating the integrated variance with a moment-matched lognormal distribution. We improve the accuracy of the numerical integration by using the Gauss–Hermite quadrature. We further obtain the option price by integrating the CEV option prices in the same manner without resorting to the small-strike volatility smile asymptotics of De Marco et al. [SIAM J. Financ. Math., 2017, 8(1), 709–737]. For the uncorrelated SABR model, the new method of option pricing is accurate and arbitrage-free across all strike prices.

Keywords: Stochastic volatility, SABR model, CEV model, Gauss–Hermite quadrature

1. Introduction

The stochastic-alpha-beta-rho (SABR) model proposed by Hagan et al. (2002) is one of the most popular stochastic volatility models adopted in the financial industry thanks to the availability of an approximate equivalent Black–Scholes (BS) volatility formula (hereafter, the HKLW formula). Despite its enormous successes, the model still poses challenges for enhancements. See Antonov et al. (2019) for an extensive literature review.

The processes for the price and volatility under the SABR model are respectively given by

$$dX_t = Y_t X_t^\beta dW_t \quad (X_0 = x_0) \quad \text{and} \quad dY_t = \nu Y_t dZ_t \quad (Y_0 = y_0), \quad (1)$$

where ν is the vol-of-vol, β is the elasticity parameter, and W_t and Z_t are the (possibly correlated) standard Brownian motions. We will denote the time-to-maturity of the option by T and the strike price by K . We also denote $\beta_* = 1 - \beta$ for simplicity.

*Corresponding author *Tel:* +86-755-2603-0568, *Address:* Rm 755, Peking University HSBC Business School, University Town, Nanshan, Shenzhen 518055, China

Email addresses: jaehyuk@phbs.pku.edu.cn (Jaehyuk Choi), malwu@ust.hk (Lixin Wu)

The uncorrelated SABR model, where W_t and Z_t are independent, draws attention thanks to the analytical tractability of the constant elasticity of variance (CEV) model,

$$dX_t = \sigma X_t^\beta dW_t \quad (X_0 = x_0).$$

Under the CEV model, the call option price¹ is given by

$$C_{\text{CEV}}(\sigma) = x_0 \bar{F}_{\chi^2} \left(\frac{K^{2\beta_*}}{\beta_*^2 \sigma^2 T}; 2 + \frac{1}{\beta_*}, \frac{x_0^{2\beta_*}}{\beta_*^2 \sigma^2 T} \right) - K F_{\chi^2} \left(\frac{x_0^{2\beta_*}}{\beta_*^2 \sigma^2 T}; \frac{1}{\beta_*}, \frac{K^{2\beta_*}}{\beta_*^2 \sigma^2 T} \right), \quad (2)$$

where $F_{\chi^2}(x; r, x')$ and $\bar{F}_{\chi^2}(x; r, x')$ are respectively the cumulative distribution function (CDF) and complementary CDF of the non-central chi-squared distribution with degrees of freedom r and non-centrality parameter x' . The formula is arbitrage free since they are obtained with the absorbing boundary condition at the origin.

The uncorrelated SABR model can be interpreted as the CEV model with a stochastic time change (Isilah, 2009). The SABR option price, for example, is the expectation of the CEV price over the average normalized integrated variance, V :

$$C_{\text{SABR}}(y_0, \nu) = \mathbb{E} \left(C_{\text{CEV}} \left(y_0 \sqrt{V} \right) \right), \quad \text{where} \quad V := \frac{1}{T} \int_0^T e^{2\nu Z_t - \nu^2 t} dt. \quad (3)$$

Here, we have omitted showing the dependency on the other variables, x_0 , β , K , and T . The probability density of V is available as an integral representation (Matsumoto and Yor, 2005, Eq. (4.1)). However, the numerical evaluation of Eq. (3) is prohibitive due to the complexity of the density function.

2. Mass at Zero using Gauss–Hermite Quadrature

Gulisashvili et al. (2018) have managed to obtain an approximation to the mass at zero, $m_{\text{SABR}} = \mathbb{P}(X_0 = 0)$ in small- and large-time limits. As “the original motivation of the paper,” they ultimately use the obtained mass at zero for the arbitrage-free implied volatility formula of De Marco et al. (2017) (hereafter, the DMHJ formula):

$$\sigma_{\text{BS}} = \frac{L}{\sqrt{T}} \left(1 + \frac{q}{L} + \frac{q^2 + 2}{2L^2} + \frac{q}{2L^3} + \dots \right) \quad \text{where} \quad L = \sqrt{2|\log(K/x_0)|} \quad \text{and} \quad q = N^{-1}(m_{\text{SABR}}), \quad (4)$$

where $N^{-1}(\cdot)$ is the inverse CDF of the standard normal distribution.

¹The put option price is given by

$$P_{\text{CEV}}(\sigma) = K \bar{F}_{\chi^2} \left(\frac{x_0^{2\beta_*}}{\beta_*^2 \sigma^2 T}; \frac{1}{\beta_*}, \frac{K^{2\beta_*}}{\beta_*^2 \sigma^2 T} \right) - x_0 F_{\chi^2} \left(\frac{K^{2\beta_*}}{\beta_*^2 \sigma^2 T}; 2 + \frac{1}{\beta_*}, \frac{x_0^{2\beta_*}}{\beta_*^2 \sigma^2 T} \right)$$

[Gulisashvili et al. \(2018\)](#) express the mass at zero as a similar expectation over the distribution of V ,

$$m_{\text{SABR}}(y_0, \nu) = \mathbb{E} \left(m_{\text{CEV}} \left(y_0 \sqrt{V} \right) \right),$$

where the mass at zero under the CEV model is given by

$$m_{\text{CEV}}(\sigma) = \bar{\Gamma} \left(\frac{x_0^{2\beta_*}}{2\beta_*^2 \sigma^2 T}; \frac{1}{2\beta_*} \right) \quad \text{for} \quad \bar{\Gamma}(x; a) = \bar{F}_{\chi^2}(2x; 2a, 0) = \frac{1}{\Gamma(a)} \int_x^\infty t^{a-1} e^{-t} dt. \quad (5)$$

The function $\bar{\Gamma}(x; a)$ is the complementary CDF of the gamma distribution² with the shape parameter a . In small-time limit, [Gulisashvili et al. \(2018\)](#) cleverly approximate V by a lognormal random variable through matching the first two moments, μ_1 and μ_2 :

$$V \approx \mu_1 \exp \left(\lambda Z - \frac{\lambda^2}{2} \right) \quad \text{for} \quad \lambda = \sqrt{\log \left(\frac{\mu_2}{\mu_1^2} \right)}.$$

The first two moments of V and, therefore, λ , are analytically available as

$$\mu_1 = \frac{(w-1)}{\nu^2 T}, \quad \mu_2 = \frac{(w^6 - 6w + 5)}{15\nu^4 T^2}, \quad \text{and} \quad \lambda = \sqrt{\log \left(\frac{w^4 + 2w^3 + 3w^2 + 4w + 5}{15} \right)} \quad \text{for} \quad w = e^{\nu^2 T}.$$

[Gulisashvili et al. \(2018\)](#), however, do not specify the method of numerical integration.

Here, we employ the Gauss–Hermite quadrature (GHQ) ([Abramowitz and Stegun, 1972](#), p. 890) for more accurate integration. Let $\{z_k\}$ and $\{w_k\}$ for $k = 1, \dots, n$ be the points and weights, respectively, of the GHQ, which then can exactly evaluate the expectation of the polynomials up to the order of $2n - 1$ with respect to the standard normal distribution. Using $\{w_k\}$ and $\{z_k\}$, the mass at zero is approximated as the weighted sum:

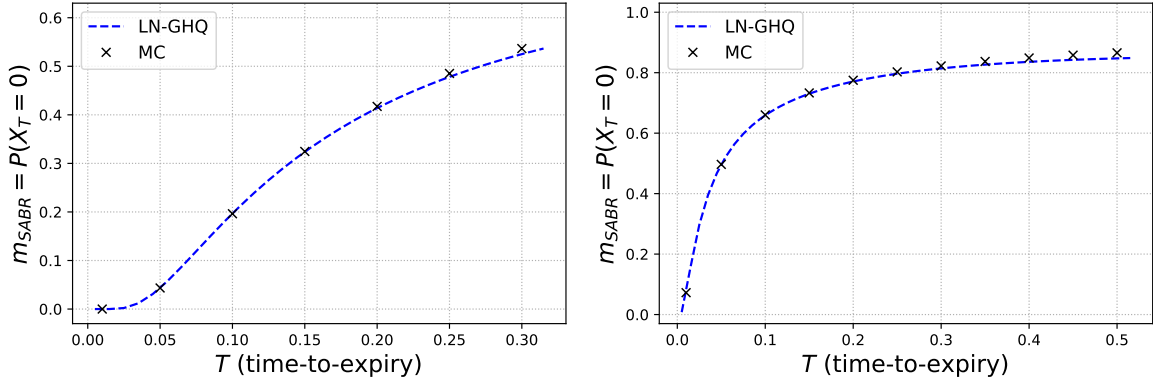
$$m_{\text{SABR}}(y_0, \nu) \approx \sum_{k=1}^n w_k m_{\text{CEV}}(y_0 \sqrt{v_k}) \quad \text{for} \quad v_k = \mu_1 \exp \left(\lambda z_k - \frac{\lambda^2}{2} \right).$$

We demonstrate the performance of our method with numerical examples. For accuracy benchmarking, we implement the Monte-Carlo method as well. We draw random values of V by simulating the paths of Y_t over the discretized time steps and integrating the values with Simpson’s method. In [Figure 1](#), we redo³ [Figure 2](#) of [Gulisashvili et al. \(2018\)](#). [Figure 1](#) shows that the mass at zero computed with GHQ (labeled as LN-GHQ) is very close to the Monte-Carlo benchmark values, and it is much closer to the benchmark than the ‘LN approx’ graph is in [Figure 2](#) of [Gulisashvili et al. \(2018\)](#). Our method also

²This is equivalent to the upper incomplete gamma function normalized by the gamma function $\Gamma(a)$.

³In [Gulisashvili et al. \(2018\)](#), x_0 is not provided. We guess $x_0 = 0.03$ based on the ‘Exact’ graph in the reference.

Figure 1: The mass at zero, m_{SABR} , as a function of time to maturity, T . We test $(x_0, y_0, \nu) = (0.03, 0.6, 1)$, and $\beta = 0.5$ (left) and $\beta = 0.3$ (right). We use $n = 10$ Gauss–Hermite quadrature points.



preserves the monotonicity of the mass at zero as T increases. Consequently, we do not see the need for the ‘small-time’ and ‘hybrid’ approaches introduced in [Gulisashvili et al. \(2018\)](#). The convergence of the GHQ is known to be very fast. We used merely $n = 10$ GHQ points for Figure 1. The errors from the converged values, evaluated with $n = 100$, are in the orders of 10^{-9} and 10^{-7} , respectively, for the two examples. See also [Choi and Wu \(2019\)](#) for another numerical example and comparisons with other methods estimating the mass at zero.

3. Option Price as an Integral of the CEV Option Price

Moreover, we can also evaluate the option price under the SABR model, Eq. (3), by GHQ. Using the GHQ, the price can be approximated by the weighted sum of those of the CEV option price, Eq. (2):

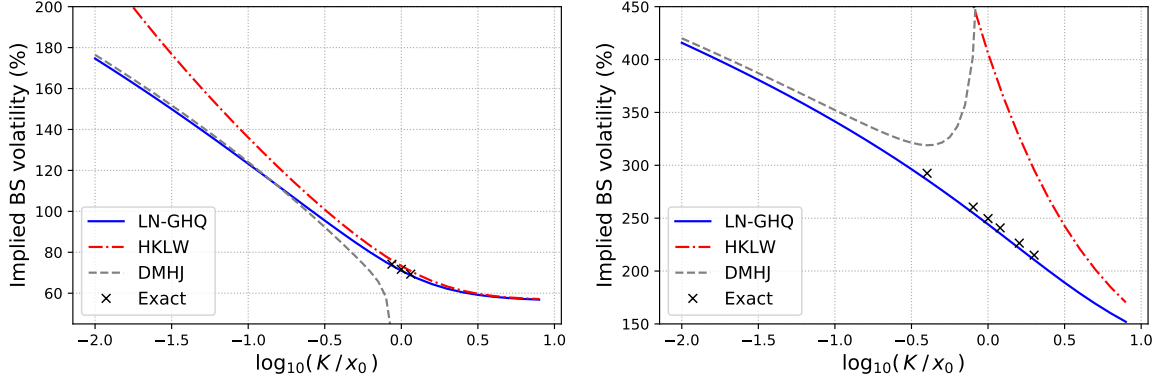
$$C_{\text{SABR}}(y_0, \nu) \approx \sum_{k=1}^n w_k C_{\text{CEV}}(y_0 \sqrt{v_k}) \quad \text{for} \quad v_k = \mu_1 \exp\left(\lambda z_k - \frac{\lambda^2}{2}\right). \quad (6)$$

This direct pricing approach has several critical advantages over the original method using the DMHJ formula. First, we can price the options for any strike price, while the DMHJ formula is accurate only for small strike and diverges for bigger strikes. Second, the price from the new method is completely arbitrage-free because so is each of the CEV price component. Third, this approach can be applied to the lognormal ($\beta = 1$) and normal ($\beta = 0$) SABR models, to which the DMHJ formula is not applicable because the mass at zero is not available.⁴ In those two cases, the CEV price formula in Eq. (6) is replaced by the Black–Scholes and Bachelier formulae, respectively.

Figure 2 demonstrates the advantages of the direct pricing method. We examine two parameter

⁴In the lognormal SABR model, the origin is an unreachable boundary. In the normal SABR model, the origin is not a boundary as the price can go negative. See [Antonov et al. \(2015\)](#) and [Choi et al. \(2019\)](#) for more detail on the normal SABR model.

Figure 2: The Black-Scholes volatility smile as a function of log strike price for two parameter sets: $(x_0, y_0, \nu, \beta, T) = (0.5, 0.5, 0.4, 0.5, 2)$ (left) and $(x_0, y_0, \nu, \beta, T) = (0.05, 0.4, 0.6, 0.3, 1)$ (right). The mass at zero, estimated by the method of this study, are $m_{\text{SABR}} = 0.1657$ and 0.7624 , respectively.



sets tested by prior studies, von Sydow et al. (2019) and Cai et al. (2017). The exact options prices are available from the references. We also compare the HKLW formula (labeled as HKLW) as it is the industry standard.⁵ The lognormal approximation with GHQ (labeled as LN-GHQ) shows an excellent agreement with the true implied volatilities near the money. In the second parameter set (right), the HKLW formula significantly deviates from the true value. In the low-strike region, the volatility smile from our method is consistent with those by the DMHJ formula, with estimated mass at zero, $m_{\text{SABR}} = 0.1657$ (left) and 0.7624 (right), respectively. These are very close from the values from the Monte-Carlo method, $m_{\text{SABR}} = 0.1634$ (left) and 0.7758 (right) respectively. Yet, not surprisingly, the DMHJ formula diverges near the money ($K = x_0$). Therefore, our new pricing method is superior to the existing method across all strike range.

References

- Abramowitz, M., Stegun, I.A. (Eds.), 1972. Handbook of Mathematical Functions. New York.
- Antonov, A., Konikov, M., Spector, M., 2015. The free boundary SABR: Natural extension to negative rates. Risk 2015, 1–6. URL: <https://ssrn.com/abstract=2557046>.
- Antonov, A., Konikov, M., Spector, M., 2019. Modern SABR Analytics. SpringerBriefs in Quantitative Finance, Cham. doi:10.1007/978-3-030-10656-0.
- Cai, N., Song, Y., Chen, N., 2017. Exact Simulation of the SABR Model. Operations Research 65, 931–951. doi:10.1287/opre.2017.1617.
- Choi, J., Liu, C., Seo, B.K., 2019. Hyperbolic normal stochastic volatility model. Journal of Futures Markets 39, 186–204. doi:10.1002/fut.21967.
- Choi, J., Wu, L., 2019. The equivalent constant-elasticity-of-variance (CEV) volatility of the stochastic-alpha-beta-rho (SABR) model. arXiv:1911.13123 [q-fin] URL: <http://arxiv.org/abs/1911.13123>, arXiv:1911.13123.

⁵For other advanced volatility approximation methods, see Choi and Wu (2019).

- De Marco, S., Hillairet, C., Jacquier, A., 2017. Shapes of Implied Volatility with Positive Mass at Zero. *SIAM Journal on Financial Mathematics* 8, 709–737. doi:[10.1137/14098065X](https://doi.org/10.1137/14098065X).
- Gulisashvili, A., Horvath, B., Jacquier, A., 2018. Mass at zero in the uncorrelated SABR model and implied volatility asymptotics. *Quantitative Finance* 18, 1753–1765. doi:[10.1080/14697688.2018.1432883](https://doi.org/10.1080/14697688.2018.1432883).
- Hagan, P.S., Kumar, D., Lesniewski, A.S., Woodward, D.E., 2002. Managing Smile Risk. *Wilmott Magazine* 2002, 84–108.
- Islah, O., 2009. Solving SABR in Exact Form and Unifying it with LIBOR Market Model. *SSRN Electronic Journal* doi:[10.2139/ssrn.1489428](https://doi.org/10.2139/ssrn.1489428).
- Matsumoto, H., Yor, M., 2005. Exponential functionals of Brownian motion, I: Probability laws at fixed time. *Probability Surveys* 2, 312–347. doi:[10.1214/154957805100000159](https://doi.org/10.1214/154957805100000159).
- von Sydow, L., Milovanović, S., Larsson, E., In't Hout, K., Wiktorsson, M., Oosterlee, C.W., Shcherbakov, V., Wyns, M., Leitao, A., Jain, S., Haentjens, T., Waldén, J., 2019. BENCHOP - SLV: The BENCHmarking project in Option Pricing – Stochastic and Local Volatility problems. *International Journal of Computer Mathematics* 96, 1910–1923. doi:[10.1080/00207160.2018.1544368](https://doi.org/10.1080/00207160.2018.1544368).